J Mater Sci (2011) 46:2778–2788
DOI 10.1007/s10853-010-5152-6

Organophosphorus and DGEBA resins containing clay nanocomposites: flame retardant, thermal, and mechanical properties

P. Sudhakara · P. Kannan · K. Obireddy · A. Varada Rajulu

Received: 27 September 2010 / Accepted: 2 December 2010 / Published online: 6 January 2011

Abstract Flame-retardant nanocomposites were prepared from diglycidylphenylphosphate (DGPP) and modified montmorillonite (MMT) clay blended with DGEBA in different ratio. T_g of all formulations increased with increasing clay content in the respective series while decreasing with increasing DGPP content. The TGA, LOI, and UL-94 data of all nanocomposites indicated that the materials were thermally stable with high flame retardancy resulting from synergetic effect of phosphorus and inorganic clay. The XRD analysis of the nanocomposites with 1 and 2% of clay indicated the intercalation of clay while rest of the samples displayed exfoliation at high clay content. As compared to neat epoxy system, a maximum increase of 59.3, 45.5, and 93% of tensile, flexural, and impact strengths were observed for the prepared nanocomposites. The SEM analysis of the failure surfaces of all DGPP containing samples showed rough with ridge patterns and river markings on the fracture surface that serves in improving the mechanical properties.

Introduction

Epoxy resins have played an important role in polymer matrix composite materials because of their superior mechanical and adhesive properties. They have been used widely as a matrix to hold high-performance fiber reinforcement together in composite materials, as well as structural adhesives [1–3]. However in many applications, e.g., structural materials for aircraft, motor vehicle construction, and electronics the common epoxy resin system cannot satisfy high thermal and flame-retardant requirements. Several approaches were attempted to modify these drawbacks. Among them, halogenation and phosphorylation methods are commonly applied to improve thermal and flame-retardant properties of epoxy resins, either by blending or chemical modification. The halogenated compounds becoming much less favored owing to their toxic gas emission, while organophosphorus compounds were found to generate less toxic plumes than halogen-containing compounds and exhibiting good flame-retardant property [4]. Phosphorus-containing oxirane compounds or curing agents in epoxy resin-based thermosets found to be more effective for many flame-retardant applications [5–14]. In our earlier study, we have synthesized, phosphorus-containing epoxy resin namely diglycidylphenylphosphate (DGPP) and utilized it for the preparation of organophosphorus liquid crystalline thermosets [15].

The layered silicates, such as montmorillonite (MMT), are increasingly being used as reinforcement in polymer composites owing to their high aspect ratio, platy morphology, and low cost. Especially modified MMT was used to improve the mechanical properties of epoxy resin thermosetting polymers in many research works [1, 16–29]. The fire retardancy of polymer–clay nanocomposites was studied by various researchers [30–34]. However, it was found that such clay additions were not themselves sufficiently effective to be classified as flame retardants. It is also possible that the combination of inorganic materials (such as nanoclay) in combination with other forms of flame-retardant additive may be more effective. In this

P. Sudhakara · P. Kannan (✉)
Department of Chemistry, Anna University,
Chennai 600025, Tamil Nadu, India
e-mail: pakannan@annauniv.edu

K. Obireddy · A. Varada Rajulu
Department of Polymer Science and Technology,
Sri Krishnadevaraya University, Anantapur 515055,
Andhra Pradesh, India

context, we have chosen DGPP as a flame retarding moiety in combination with modified MMT in varying weight percentages and blended with DGEBA without sacrificing the mechanical properties of final cured products. The aliphatic polyamine (TETA) was used as an ambient temperature hardener. The effect of DGPP and clay content on thermal and mechanical properties was investigated.

Experimental

Materials

Phosphorus-containing DGPP was synthesized according to the reported procedure [15]. The surfactant cetyltrimethylammonium bromide [$CH_3(CH_2)15$ N(CH3)3Br] and NaCl were purchased from SRL chemical company (India). The MMT was purchased (Aldrich chemicals) and modified using appropriate procedure [16]. Epoxy resin (DGEBA; Araldite LY 556) with equivalent weight per epoxide group of 195 ± 5 and ambient temperature hardener TETA (HY 951) were purchased from Ciba Geigy.

Fabrication of clay nanocomposites

A known amount of DGEBA and various percentages (5, 10, and 15) of DGPP and modified clay (1, 2, 3, and 4) were thoroughly mixed at 70 °C by mechanical stirring followed by ultrasonic mixing for 20 min and cooled to room temperature. Then a stoichiometric amount of curing agent was added and mixed mechanically for 5 min, the mixture was degassed again and poured into a glass mold covered by Teflon sheet having dimensions of 160 mm x 160 mm x 3 mm. The composites were cured for 48 h at 75 °C and post-cured for 4 h at 135 °C.

Thermal properties

Curing studies and determination of glass transition temperature of the samples were performed on a DSC instrument (DuPont 910) at a heating rate of 10 °C/min, sample weight of about 3–5 mg, under nitrogen atmosphere in the temperature range 35–300 °C. Thermogravimetric analysis was used to analyze the thermal stability of cured composites using a TA 3000 thermal analyzer in a dry nitrogen atmosphere at a heating rate of 20 °C/min. Sample of approximately 5 mg was placed in the crucible and heated from 35–700 °C with constant heating rate of 20 °C.

Mechanical properties

Tensile and flexural tests were carried out on a standard computerized INSTRON 3369 Universal testing machine. Tensile test was conducted at a cross-head speed of 5 mm/min according to ASTM D 3039-76 using 150 mm x 25 mm x 3 mm specimen. The flexural strength of the samples was measured according to ASTM D5943-96 at a cross-head speed of 2 mm/min using three-point flexural tests. The specimen was 100 mm x 15 mm x 3 mm was measured according to ASTM D5943-96 in the three point loading mode. The impact test was performed using an Izod impact testing machine, supplied by International equipments, Mumbai and India. Rectangular strips of 122 mm × 13 mm × 3 mm were used according to ASTM 256-88 specifications. The impact test was carried out at room temperature and impact energy was reported in Jm^{-1}. Five test samples were used for each test and average value were reported. The glass transition temperature (T_g) of the nanocomposites were conformed with dynamic mechanical analysis (DMA) by DMA 2940 (TA Instruments). The analyses were performed at a frequency of 1 Hz and a temperature range of 30–250 °C at a heating rate of 5 °C/min. The T_g value was taken to be the temperature at the maximum of the tanδ peak.

Morphology

Morphology of fractured surface of samples was examined using a scanning electron microscope (SEM; JEOL JSM Model 6360). The fractured surface of the samples was sputter coated with gold (JEOL JFC-1600) an Auto Fine Coater prior to the fractographic examination.

X-ray diffraction study

X-ray diffraction patterns of powdered samples of neat epoxy and its nanocomposites were studied using a Philips PW 1820 diffractometer. Nickel-filtered Cu Kα radiation (radiation wavelength, $\lambda = 0.154$ nm) was produced by a PW1729 X-ray generator at an operating voltage of 40 kV and a current of 30 mA. The scanning angle, 2θ, for all the experiments was kept between 0.2° and 10° with a step size 0.5°.

Results and discussion

Sixteen samples were prepared for this investigation (Scheme 1) and named as A1–A4 (DGEBA–1–4% clay), B1–B4 (DGEBA–5% DGPP–1–4% clay), C1–C4 (DGEBA–10% DGPP–1–4% clay) and D1–D4 (DGEBA–15% DGPP–1–4% clay). These samples were analyzed and discussed.

DSC analysis

The samples were subjected to DSC analysis to identify the completion of curing process and glass transition

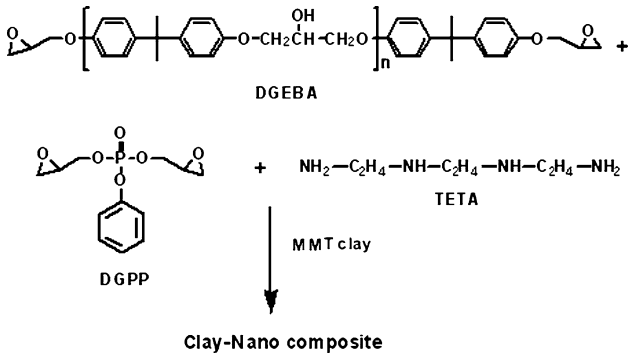

Scheme 1 Synthesis of clay nanocomposites

temperatures, and the data is presented in Table 1. The representative DSC thermograms are shown in Fig. 1a and b. The thermograms indicated that no residual peak was observed after curing the samples at 75 °C for 48 h and post-curing at 135 °C for 4 h. The data indicates that T_g of all formulations increased with increasing clay content from 1 to 4% in the respective series. The T_g of the formulation A1–A4 and B1–B4 are higher than the neat epoxy resins. The increase in glass transition temperature of nanocomposite system was attributed the dispersion of silicate layers of clay and their ability to hinder the motion of molecular chain and network junctions [35]. It may be defined that as the clay concentration increased, more polymer–clay interactions occur, resulting in immobilization of part of resin matrix and ultimately reduces the free volume. These restrictions hinder the relaxation mobility of polymer segments near the interface, leading to an increase in T_g [36]. However, when compared with neat epoxy system, the T_g of formulations of C1–C4 and D1–D4 were slightly decreased with increasing DGPP content from 10 to 15% attributed to the plasticizing effect of DGPP with increasing concentration arises by weaker P–O–C bond that can dominate the clay effect. The low concentration and good interaction of DGPP with clay and DGEBA, the T_g values of formulations B1–B4 were reasonably higher than the neat epoxy system. Further the T_g values obtained by DSC were conformed with the values obtained by DMA analysis (Table 1).

Thermal stability and flame-retardant properties

In order to find the effect of addition of phosphorus and clay, and their combination on thermal stability of cured nanocomposites, thermogravimetric experiments were performed and the representative thermograms are shown in Fig. 2a and b and data is presented in Table 1. The flame-retardant efficiency of the material can be approximately identified from the thermograms by their various stages of decomposition and understanding of char yield of the material. The temperature corresponding to 5% weight loss in thermograms was regarded as a minimum weight loss of the sample. It is inferred from the thermograms that all the samples underwent two-stage decomposition and data suggests the thermal stability of all formulations is higher than the neat epoxy system. The

Table 1 Thermal and flame-retardant properties of cured nanocomposites (A1–A4, B1–B4, C1–C4, and D1–C4)

Formulation	Formulation code	T_g (°C) (DSC)	T_g (°C) (DMA)	Weight loss		T_{max} (°C)		Char yield (%)	UL-94 (mm/min)	LOI (%)
				5%	50%	Stage 1	Stage 2			
Neat DGEBA	–	131	132	292	340	326	–	5	35	19
DGEBA–1% clay	A1	135	134	360	412	395	530	8.2	31	21.3
DGEBA–2% clay	A2	135	137	344	407	391	540	9.0	31	25.4
DGEBA–3% clay	A3	137	136	345	412	393	552	9.5	30	24.3
DGEBA–4% clay	A4	140	142	355	415	395	560	10	29	27.2
DGEBA–5% DGPP–1% clay	B1	130	131	325	385	372	550	11.2	24	29.6
DGEBA–5% DGPP–2% clay	B2	133	133	315	382	370	551	11.6	23	31.2
DGEBA–5% DGPP–3% clay	B3	135	133	305	382	368	553	12.3	21	30.6
DGEBA–5% DGPP–4% clay	B4	137	136	315	387	372	557	12.5	23	32.0
DGEBA–10% DGPP–1% clay	C1	118	120	313	378	360	558	12.2	21	32.1
DGEBA–10% DGPP–2% clay	C2	120	122	315	375	356	558	12.7	20	33.2
DGEBA–10% DGPP–3% clay	C3	123	124	305	381	361	567	14.5	20	33.6
DGEBA–10% DGPP–4% clay	C4	128	130	324	376	357	568	15.2	19	33.9
DGEBA–15% DGPP–1% clay	D1	110	111	322	374	358	562	17.4	18	31.2
DGEBA–15% DGPP–2% clay	D2	115	113	311	374	355	565	18.6	17	33.3
DGEBA–15% DGPP–3% clay	D3	115	114	296	375	357	577	22.1	17	35.1
DGEBA–15% DGPP–4% clay	D4	118	119	295	375	357	578	23.5	15	34.5

increase in thermal stability is ascribed to the presence of nanoclay layers in the epoxy, which acts as a physical barrier preventing evolution of volatile degradation products generated during decomposition of the matrix [37]. Usually the presence of phosphorus content (DGPP) reduces thermal stability of neat epoxy resin referable to the plasticizing effect of DGPP which was also observed in our recent studies for DGEBA resin, blended with 5, 10, and 15% DGPP decreasing thermal stability (neat epoxy 292 °C; DGEBA–5% DGPP 288 °C; DGEBA–10% DGPP 274 °C; DGEBA–15% DGPP 268 °C). However, the incorporation of clay overcomes the effect of DGPP on thermal stability of DGEBA and no abrupt change was observed even with 15% addition of DGPP. It was also observed from the data (Table 1) of thermograms that thermal stability of all samples decreased slightly in respective series with increase in clay concentration from 1 to 4% attributed to the decomposition of organic part (alkyl ammonium chains) of modified clay [38]. The phosphorus–clay formulations (B1–B4, C1–C4, and D1–D4) were demonstrated earlier degradation than the formulations A1–A4 (neat epoxy and clay) with char yields attributed to earlier decomposition of P–O–C bonds and form a phosphorus-rich residue as layer on the material that prevent further decomposition [39]. The formation of high char yield during combustion of materials can usually limit the production of combustible carbon-containing gases and flow of oxygen and decrease the thermal conductivity of the burning materials, thus flammability gets reduced. Hence, the burning rate of DGPP containing formulations is delayed as the temperature increases while the samples obtained from neat epoxy–clay undergoes drastic degradation in the first stage [40, 41]. The char yield at 700 °C are given in Table 1, evidenced that char yield increases with increasing clay and DGPP content which can increase flame-retardant property accordingly.

To confirm the flame-retardant efficiency of all the formulations, UL94 (horizontal burning test) flammability test (Fig. 3) and limiting oxygen index (Fig. 4) test were conducted and the data is presented in Table 1. Generally, the LOI values for polymers should be >26 to meet the requirements for flame-retardant applications and specimens must not have a horizontal burning rate greater than 37 mm/min for thicknesses between 3 and 12 mm [42]. It is observed from Table 1 that the LOI values of neat epoxy–clay (A1–A4) and neat epoxy–phosphorus–clay (B1–B4, C1–C4, and D1–D4) composites were found to be 21.3–27.2 and 29.6–34.5 and horizontal burning rate values were found to be 31–29 and 24–15 mm/min, respectively. However in our earlier studies, LOI values for DGEBA–5% DGPP, DGEBA–10% DGPP, DGEBA–15% DGPP were found in the range 27–30 and 26–20 mm/min which are slightly lower than the present formulations, thus the data of TGA, LOI, and UL94 tests suggested that DGEBA–clay–DGPP nanocomposites are potentially better flame-retardant materials than DGEBA–clay system.

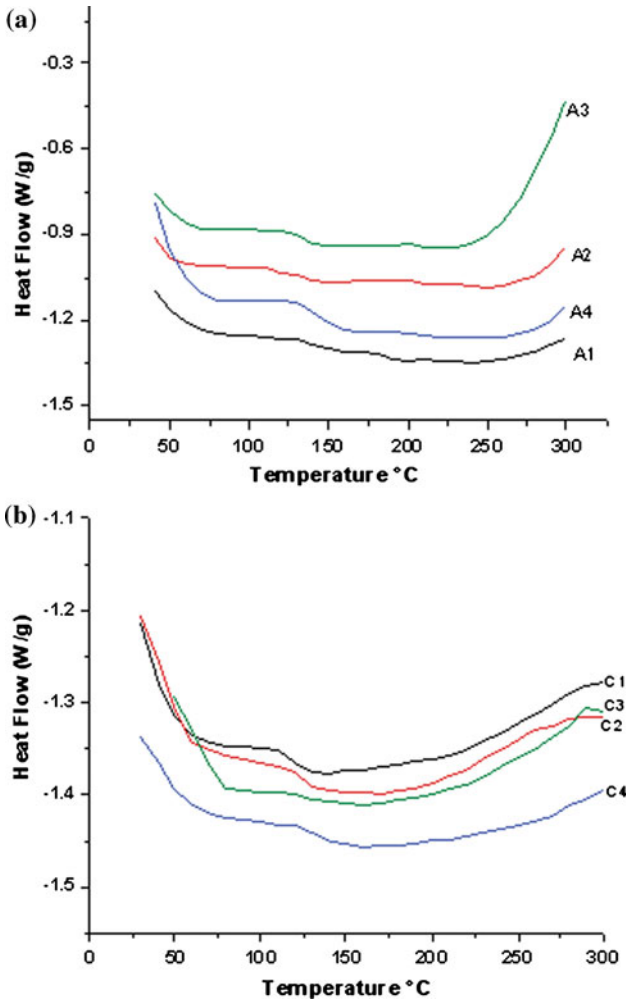

Fig. 1 DSC thermograms of cured nanocomposites **a** *A1–A4* (DGEBA–1–4% clay), **b** *C1–C4* (DGEBA–10% DGPP–1–4% clay)

X-ray diffraction study

X-ray diffraction is the most useful method to evaluate the *d*-spacing between the clay layers. The angle and *d*-spacing values are related through Bragg's law, stated in equation $n\lambda = 2d\mathrm{Sin}\theta$ where "*n*" is an integer, λ is the wavelength, θ is the glancing angle of incidence, and *d* is the interplanar spacing of the crystal [24, 43].

Figures 5 and 6 show the diffraction pattern of pristine (MMT) and modified clay and nanocomposites. Table 2 summarizes the results of SAXD analysis for clay and nanocomposites. The pristine clay (MMT; Fig. 5) for the reflection peak at $2\theta = 6.14°$ (*d*-spacing, 1.43 nm) is assigned to the (0 0 1) basal plane, which corresponds to an

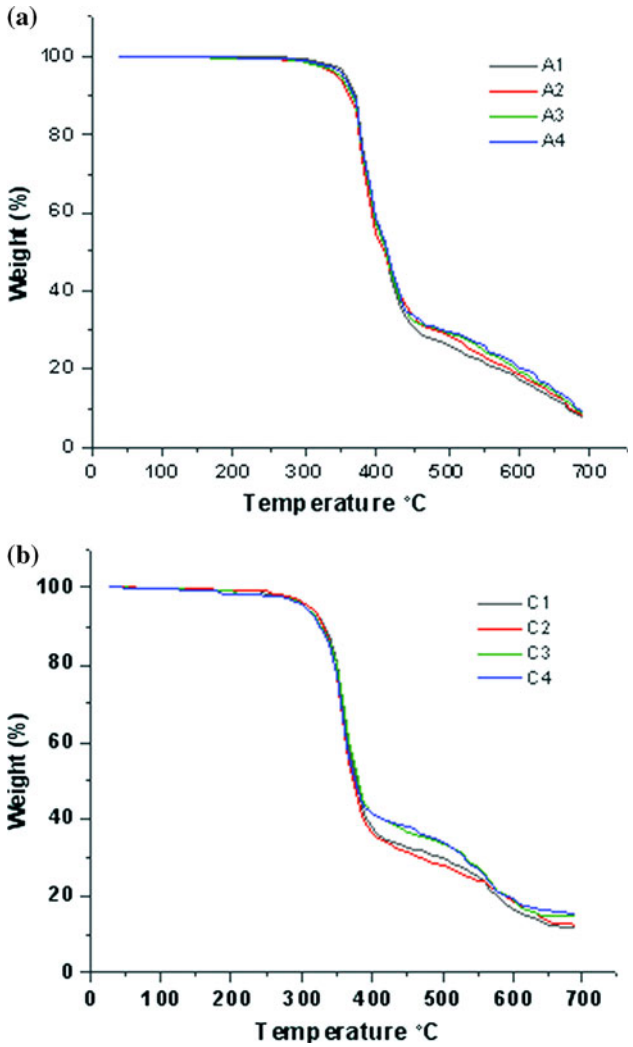

Fig. 2 TGA thermograms of cured nanocomposites **a** *A1–A4* (DGEBA–1–4% clay), **b** *C1–C4* (DGEBA–5% DGPP–1–4% clay)

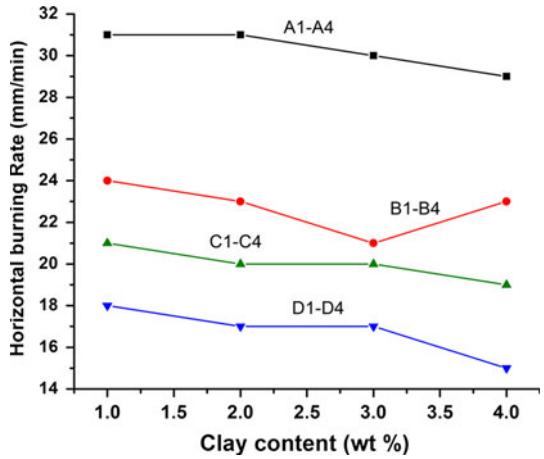

Fig. 3 Horizontal burning rate of cured nanocomposites *A1–A4* (DGEBA–1–4% clay), *B1–B4* (DGEBA–5% DGPP–1–4% clay), and *C1–C4* (DGEBA–10% DGPP–1–4% clay), and *D1–D4* (DGEBA–15% DGPP–1–4% clay)

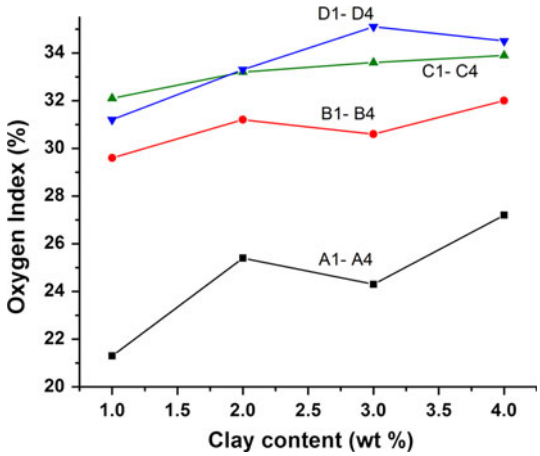

Fig. 4 Limiting oxygen index of cured nanocomposites *A1–A4* (DGEBA–1–4% clay), *B1–B4* (DGEBA–5% DGPP–1–4% clay), *C1–C4* (DGEBA–10% DGPP–1–4% clay), and *D1–D4* (DGEBA–15% DGPP–1–4% clay)

interlayer spacing of clay. After modification with CTAB, diffraction peak of the clay shifted to a new position at 4.43° (1.49 nm), corresponded to a peak of modified-MMT. The increased *d*-spacing confirmed that intercalation and surface modification of MMT had taken place. The absence of basal reflection in the samples B1, C1, C2, and D1 with 1 and 2% clay (Fig. 6) suggests the formation of an exfoliated clay structure after in situ polymerization. However, a small peak at $2\theta = 1.41$–$3.22°$ (*d*-spacing 6.21–4.53 nm) was observed for the samples with 3 and 4% nanoclay composites, respectively, probably indicating that the clay platelets are not fully exfoliated but intercalated throughout the matrix. From the XRD data (Table 2)

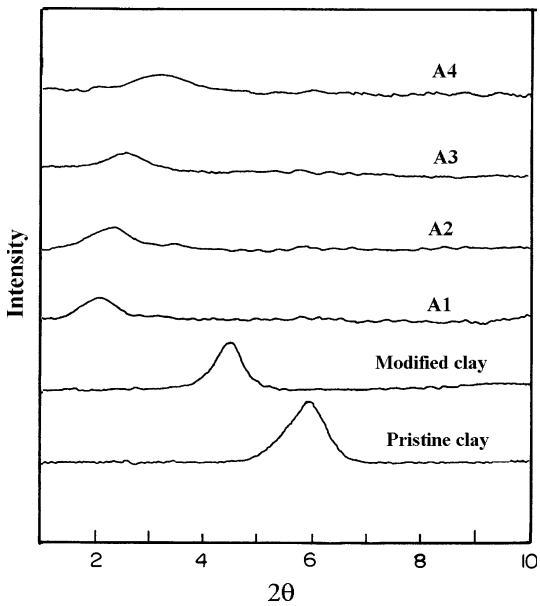

Fig. 5 XRD patterns of the pristine, modified MMT and the DGEBA–clay nanocomposites *A1–A4* (DGEBA–1–4% clay)

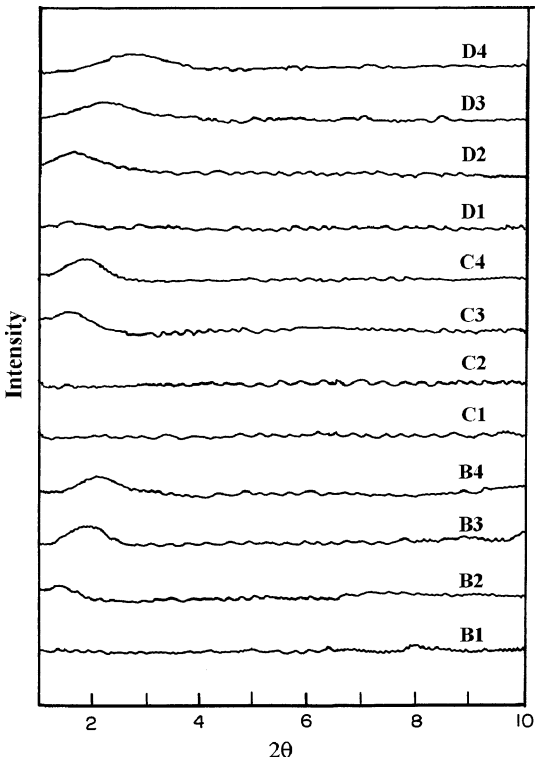

Fig. 6 XRD patterns of DGEBA–DGPP–clay nanocomposites *B1–B4* (DGEBA–5% DGPP–1–4% clay), *C1–C4* (DGEBA–10% DGPP–1–4% clay), and *D1–D4* (DGEBA–15% DGPP–1–4% clay)

of all formulations, it is concluded that the *d*-spacing values of the formulations with DGPP were higher than the DGEBA–nanoclay composites that indicates good interaction and dispersion of DGPP in DGEBA–clay system.

Mechanical properties

Tensile, Flexural, and Impact properties

Table 3 indicates the results of tensile, flexural, and impact tests and Figs. 7, 8, 9, 10, and 11 depict the tensile strength, tensile modulus, flexural strength, flexural modulus, and impact strength versus clay contents, respectively. The data revealed that except the formulation D4, tensile and flexural strength as well as modulus values of remaining formulations are higher than that of neat epoxy system. When compared to neat epoxy system, a maximum increase of 59.3% tensile strength for C2, 45.5% flexural strength for C3, and minimum increase of 4.2% tensile strength and 1.5% flexural strength were observed for D3. The tensile and flexural properties in the respective series were increased with increase in clay content from 1 to 3% and decreased slightly for 4% while increase in modulus. It is also noted that tensile strain is reduced with an increase of clay content. The improved modulus, strength, and decreased strain can be directly ascribed to stiffening effect as well as higher modulus of the clay than the epoxy resin and good dispersion of clay in the resin. However, decrease in tensile and flexural strength could be attributed the aggregation of some platelets in the nanocomposites. This allows entrapment of small air voids within the blend and

Table 2 XRD results of pristine and modified clays and (A1–A4), (B1–B4), (C1–C4), and (D1–D4)

Formulation	Formulation code	Diffraction angle	*d*-Spacing (nm) by SAXD	Morphology
Pristine clay	–	6.14	1.43	–
Modified clay	–	4.43	1.99	Intercalated
DGEBA–1% clay	A1	2.12	4.16	Intercalated
DGEBA–2% clay	A2	2.32	3.80	Intercalated
DGEBA–3% clay	A3	2.72	3.25	Intercalated
DGEBA–4% clay	A4	3.22	2.74	Intercalated
DGEBA–5% DGPP–1% clay	B1	–	–	Exfoliated
DGEBA–5% DGPP–2% clay	B2	1.41	6.21	Intercalated
DGEBA–5% DGPP–3% clay	B3	1.89	3.86	Intercalated
DGEBA–5% DGPP–4% clay	B4	2.12	4.16	Intercalated
DGEBA–10% DGPP–1% clay	C1	–	–	Exfoliated
DGEBA–10% DGPP–2% clay	C2	–	–	Exfoliated
DGEBA–10% DGPP–3% clay	C3	1.62	5.44	Intercalated
DGEBA–10% DGPP–4% clay	C4	1.87	4.72	Intercalated
DGEBA–15% DGPP–1% clay	D1	–	–	Exfoliated
DGEBA–15% DGPP–2% clay	D2	1.72	5.11	Intercalated
DGEBA–15% DGPP–3% clay	D3	2.32	3.78	Intercalated
DGEBA–15% DGPP–4% clay	D4	2.95	2.99	Intercalated

Table 3 Tensile, flexural, and impact properties of cured nanocomposites (A1–A4, B1–B4, C1–C4, and D1–D4)

Formulation	Formulation code	Tensile strength (MPa)	Tensile modulus (GPa)	Strain (%)	Flexural strength (MPa)	Flexural modulus (GPa)	Impact strength (J/m)
Neat DGEBA	–	40.6	2.00	2.62	74.5	2.61	46
DGEBA–1% clay	A1	50.3	2.603	2.60	76.2	2.71	38.12
DGEBA–2% clay	A2	53.1	2.622	2.217	78.5	2.76	35.32
DGEBA–3% clay	A3	53.8	2.934	2.33	81.3	2.957	31.311
DGEBA–4% clay	A4	48.2	3.287	1.812	75.8	3.61	30.61
DGEBA–5% DGPP–1% clay	B1	55.4	2.522	2.51	88.2	2.32	49.31
DGEBA–5% DGPP–2% clay	B2	56.2	2.811	2.48	95.4	2.58	49.94
DGEBA–5% DGPP–3% clay	B3	57.1	2.84	2.24	97.6	2.812	48.33
DGEBA–5% DGPP–4% clay	B4	56.4	2.95	2.21	90.4	2.91	47.95
DGEBA–10% DGPP–1% clay	C1	62.4	2.67	2.91	102.2	2.561	58.71
DGEBA–10% DGPP–2% clay	C2	64.7	2.69	2.65	104.1	2.387	54.23
DGEBA–10% DGPP–3% clay	C3	62.8	2.718	2.11	108.5	2.733	54.56
DGEBA–10% DGPP–4% clay	C4	59.1	2.91	2.12	94.2	2.63	52.87
DGEBA–15% DGPP–1% clay	D1	52.4	2.092	3.52	78.9	2.231	57.45
DGEBA–15% DGPP–2% clay	D2	47.1	2.214	3.45	83.2	2.35	58.92
DGEBA–15% DGPP–3% clay	D3	42.3	2.42	2.84	75.6	2.421	50.31
DGEBA–15% DGPP–4% clay	D4	40.1	2.453	2.73	69.2	2.456	48.65

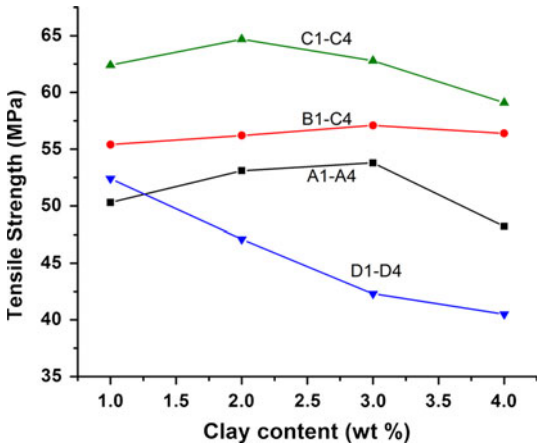

Fig. 7 Tensile strength versus clay content of cured nanocomposites *A1–A4* (DGEBA–1–4% clay), *B1–B4* (DGEBA–5% DGPP–1–4% clay), *C1–C4* (DGEBA–10% DGPP–1–4% clay), and *D1–D4* (DGEBA–15% DGPP–1–4% clay)

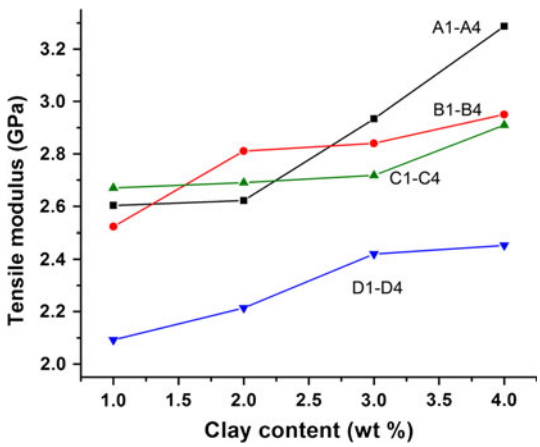

Fig. 8 Tensile modulus versus clay content of cured nanocomposites *A1–A4* (DGEBA–1–4% clay), *B1–B4* (DGEBA–5% DGPP–1–4% clay), *C1–C4* (DGEBA–10% DGPP–1–4% clay), and *D1–D4* (DGEBA–15% DGPP–1–4% clay)

also causes a poor dispersion resulting in the formation of agglomerates/tactoids in the epoxy matrix [1].

On the other hand, when the addition of DGPP is concerned, the mechanical properties of all the formulations were affected. The tensile and flexural properties were improved about 4.2–59.3 and 1.5–45.5%, respectively, attributed to the –P=O group in DGPP is more polar in nature and it can form hydrogen bond with residual OH groups generated in the curing process, this serves in good compatibility of DGPP resin with DGEBA that in turn act as crack stoppers and increases tensile and flexural strength as well as modulus. The tensile and flexural properties of B1–B4, C1–C4 are increased with increase in DGPP content; however, their increase slow down as the amount of DGPP increased to 15%, because of the lower bond strength of P–O–C bonds in DGPP provide more flexibility and plasticizing effect to the cured system, thus rigidity of system will be reduced.

In general, the impact strength decreases with increasing clay content as observed in Fig. 11 for A1–A4. The

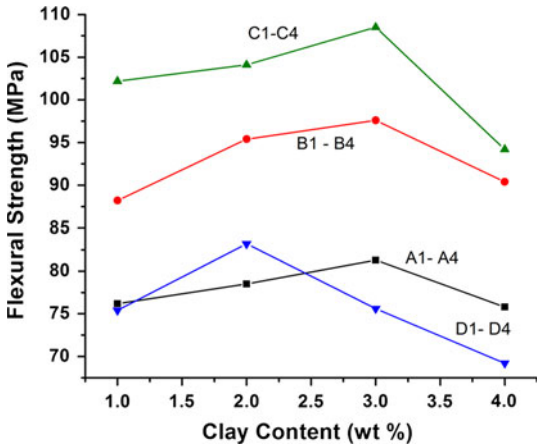

Fig. 9 Flexural strength versus clay content of cured nanocomposites *A1–A4* (DGEBA–1–4% clay), *B1–B4* (DGEBA–5% DGPP–1–4% clay), *C1–C4* (DGEBA–10% DGPP–1–4% clay), and *D1–D4* (DGEBA–15% DGPP–1–4% clay)

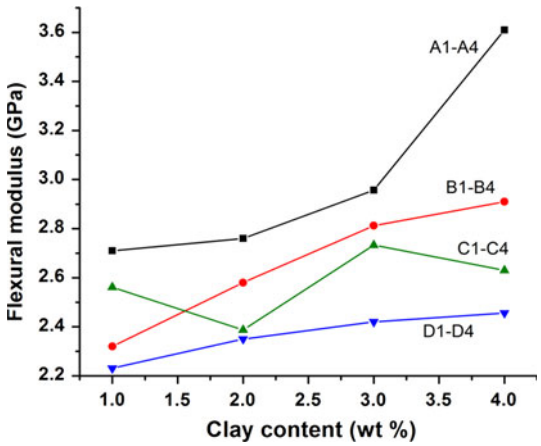

Fig. 10 Flexural modulus versus clay content of cured nanocomposites *A1–A4* (DGEBA–1–4% clay), *B1–B4* (DGEBA–5% DGPP–1–4% clay), *C1–C4* (DGEBA–10% DGPP–1–4% clay), and *D1–D4* (DGEBA–15% DGPP–1–4% clay)

addition of phosphorus resin (DGPP) into DGEBA and clay system greatly increases the impact strength of B1–B4, C1–C4, and D1–D4, in comparison to impact strength of the samples containing neat epoxy and clay content of 1–4% (A1–A4) and moderate increase as compared to neat epoxy resin system. Among the three series (B1–B4, C1–C4, and D1–D4), the formulations of the C1–C4 and D1–D4 series exhibited good impact strength resulting from toughening effect with increasing amount of DGPP.

SEM analysis

Morphologies of fractured surfaces of tensile tested nanocomposites were studied under scanning electron microscopy (SEM) and the representative SEM photographs depicted in Fig. 12a–h. An uniform distribution of clay in

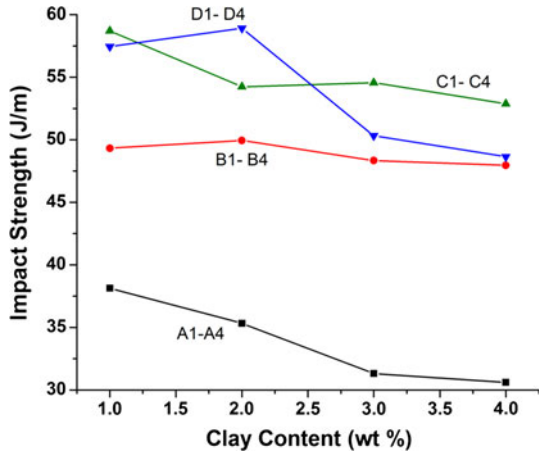

Fig. 11 Impact strength versus clay content of cured nanocomposites *A1–A4* (DGEBA–1–4% clay), *B1–B4* (DGEBA–5% DGPP–1–4% clay), *C1–C4* (DGEBA–10% DGPP–1–4% clay), and *D1–D4* (DGEBA–15% DGPP–1–4% clay)

DGEBA and homogeneous fractured surface of A1 with 1% clay indicated Fig. 12a. The homogenous distribution of clay helps as a good reinforcement, hence tensile and flexural strength as well as modulus of the material increased while impact strength decreased compared to neat epoxy system as showed in Table 2. Figure 12b evidences the fracture surface of A4 in which the clay particles agglomerate as the clay concentration increases and act as stress concentrators while decreasing impact strength. When the micrographs of nanocomposites with clay 1, and 2% (Fig. 12a, e, c, g) and with clay 4% (Fig. 12a, h) are compared, it can be seen that at the 1, 2, and 3% clay content exhibit better dispersion and a lower degree of agglomeration than nanocomposites with 4% clay. Agglomerates give rise to lower clay–polymer surface interactions and higher stress concentrations. In general, both of these factors lead to lower mechanical properties of the nanocomposites. On the other hand, smaller agglomerates and higher exfoliation of the clay result in highly improved mechanical properties.

Since the compatibility can be increased by hydrogen bonding between DGPP and DGEBA phases, distribution of DGPP network becomes more homogeneous, resulting in well-dispersed domains leads to improve the mechanical properties of all the DGPP-containing nanocomposites (B1–B4, C1–C4, and D1–D4). The failure surface of all DGPP-containing samples exhibit rough with ridge patterns, and river markings could also be seen on the fracture surface. As it can be observed from Fig. 12c–h, the roughness of the samples was increased with increasing DGPP content. The roughness of the fracture surface was ascribable to two reasons. First, it is an indication of crack path deflection. Second, the roughness indicated the ductile

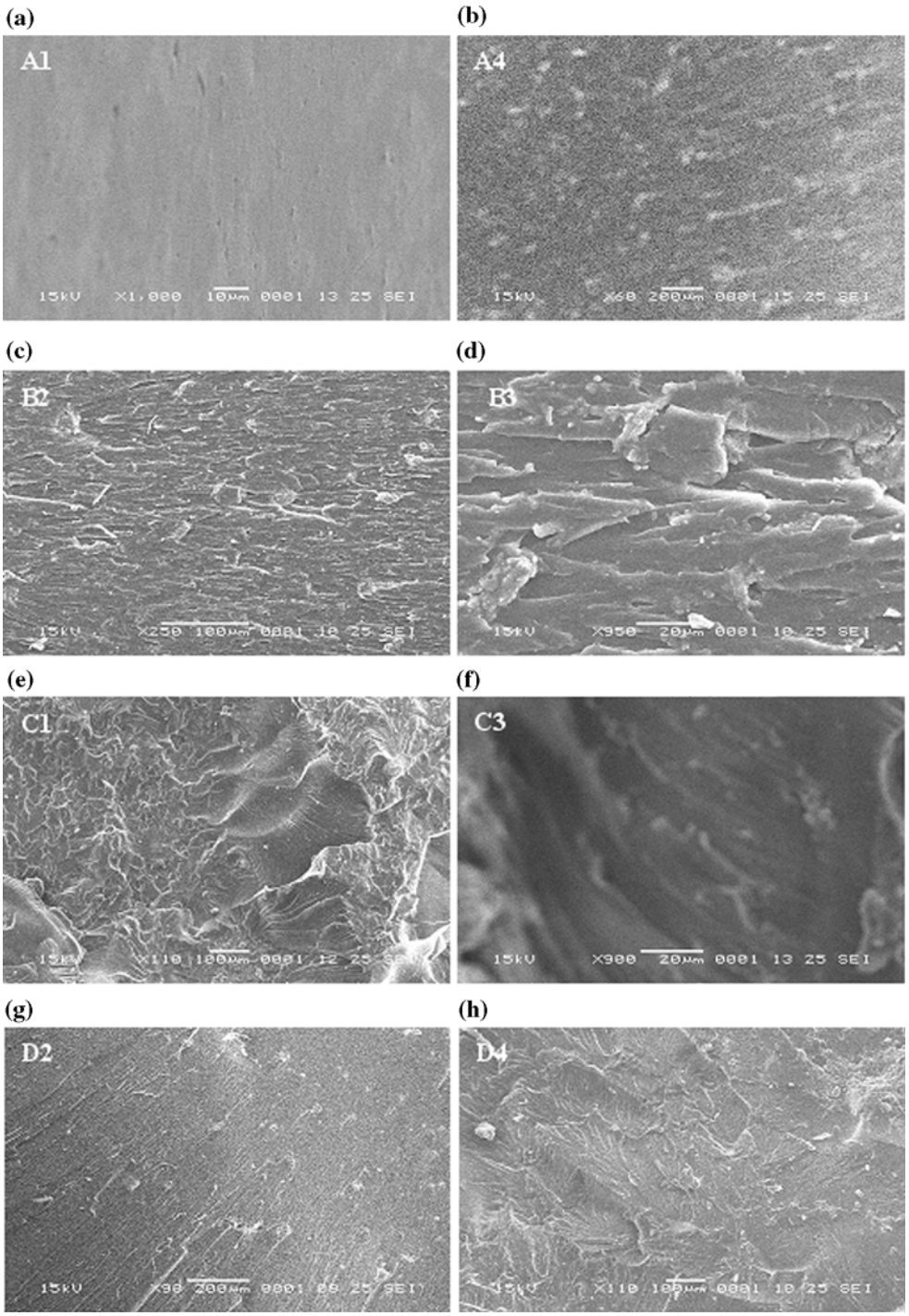

Fig. 12 SEM photographs of **a** *A1* (DGEBA–1% clay), **b** *A4* (DGEBA–4% clay), **c** *B2* (DGEBA–5% DGPP–2% clay), **d** *B3* (DGEBA–5% DGPP–3% clay), **e** *C1* (DGEBA–10% DGPP–1% clay), **f** *C3* (DGEBA–10% DGPP–3% clay), **g** *D2* (DGEBA–15% DGPP–2% clay), **h** *D4* (DGEBA–15% DGPP–4% clay)

nature of the crack [27]. The matrix became less brittle in comparison with the DGEBA–clay (A1–A4) formulations because of the flexible nature of DGPP. Another factor responsible for improved mechanical properties with addition of DGPP was local plastic deformation of the matrix. The dispersed domains were acted as stress concentrators, and this led to the plastic deformation of the matrix surrounding the domains. As reported by Hedrick et al. [44], river markings on the fracture surface were an indication of plastic deformation of the matrix.

Conclusions

The flame-retardant nanocomposites by utilizing synergetic effect of phosphorus from diglycidylphenylphosphate (DGPP) and modified-MMT mixing with DGEBA in various ratios were developed. Sixteen formulations were prepared and named as A1–A4 (DGEBA-1–4% clay), B1–B4 (DGEBA–5% DGPP–1–4% clay), C1–C4 (DGEBA–10% DGPP–1–4% clay) and D1–D4 (DGEBA–15% DGPP–1–4% clay) and tested their properties. The T_g of all formulations increased with increasing clay content from 1 to 4% in the respective series attributed to the dispersion of silicate layers of clay and their ability to hinder the motion of molecular chains and network junctions. On the other hand, the T_g was decreased with increasing DGPP content from 10 to 15% due to the plasticizing effect of P–O–C. The thermal stability of nanocomposites (360–295 °C) was greatly improved by addition of nanoclay and DGPP in comparison with neat epoxy system (292 °C). The LOI and horizontal burning rate values of all the DGEBA–DGPP–clay nanocomposites were found to be 29.6–34.5 and 24–15 mm/min, respectively, indicate good flame-retardant efficiency of the prepared nanocomposites. XRD analysis revealed that nanocomposites with 1–2% of clay exhibited exfoliation of clay while the rest of the samples evidence intercalation at higher clay content.

The tensile and flexural properties in respective series were increased with increase in clay content from 1 to 3% and decreased slightly for 4% while increase the modulus, tensile strain gets reduced with an increase of clay content. When compared to neat epoxy system, a maximum increase of 59.3, 45.5, and 93% of tensile, flexural, and impact strengths were observed for the nanocomposites. The formulations C1–C4 and D1–D4 with 10 and 15% DGPP were displayed good impact properties resulting from toughening effect with increasing amount of DGPP. SEM analysis indicates that failure surface of all DGPP-containing samples designate rough with ridge patterns and river markings on the fracture surface that helps in improving the mechanical properties. Finally, it is concluded that the results obtained by various characterization methods suggest that these nano composites are good flame-retardant material possessing superior mechanical and thermal properties.

Acknowledgements P. K gratefully acknowledges the financial support from Department of Science and Technology, New Delhi, India, under the SERC Scheme (Ref. Sanction No. SR/S1/PC-14/2003). P. S sincerely acknowledges the Council of Scientific and Industrial Research (CSIR), New Delhi, India, for the award of Senior Research Fellowship.

References

1. Qi B, Zhang QX, Bannister M, Mai YW (2006) Compos Struct 75:514
2. Lee H, Neville K (1967) Handbook of epoxy resins. McGraw-Hill, New York
3. Potter WG (1970) Epoxide resins. Springer, New York
4. Wang X, Zhang Q (2004) Eur Polym J 40:385
5. Laskoski M, Dominguez DD, Keller TM (2007) Polymer 48:6234
6. Lin CH, Hwang TY, Taso YR, Lin TL (2007) Macromol Chem Phys 208:2628
7. Liu W, Varley RJ, Simon GP (2006) Polymer 47:2091
8. Levchik S, Piotrowski A, Weil E, Yao Q (2005) Polym Degrad Stab 88:57
9. Levchik SV, Weil ED (2004) Polym Int 53:1901
10. Lin CH (2004) Polymer 45:7911
11. Perez RM, Sandler JKW, Altstädt V, Hoffmann T, Pospiech D, Ciesielski M, Döring M, Braun U, Knoll U, Schartel B (2006) J Mater Sci 41:4981. doi:10.1007/s10853-006-0134-4
12. Wang CS, Lin CH (1999) J Polym Sci A 37:3903
13. Wu CS, Liu YL, Chiu YS (2002) Polymer 43:4277
14. Perez RM, Sandler JKW, Altsta V, Hoffmann DTT, Pospiech D, Ciesielski M, Doring M (2006) J Mater Sci 41:341. doi:10.1007/s10853-005-2720-2
15. Sudhakara P, Kannan P (2009) Polym Degrad Stab 94:610
16. Xu W, Bao S, He P (2002) J Appl Polym Sci 84:842
17. Zhao Z, Gou J, Bietto S, Ibeh C, Hui D (2009) Compos Sci Technol 69:2081
18. Salahuddin N, Moet A, Hiltner A, Baer E (2002) Eur Polym J 38:1477
19. Daud W, Bersee HEN, Picken SJ, Beukers A (2009) Compos Sci Technol 69:2285
20. Wang Z, Pinnavaia TJ (1998) Chem Mater 10:1820
21. Pradip KM, Prasanta KG, Anil KB (2009) J Mater Sci 44:5861. doi:10.1007/s10853-009-3827-7
22. Ahmadi SJ, Huang YD, Li W (2004) J Mater Sci 39:919. doi:10.1023/B:JMSC.0000017753.90222.96
23. Wang K, Chen L, Wu J, Toh ML, He C, Yee AF (2005) Macromolecules 38:788
24. Basara C, Yilmazer U, Bayram G (2005) J Appl Polym Sci 98:1081
25. Yang JP, Yang G, Xu G, Fu SY (2007) Compos Sci Technol 67:2934
26. Fu T, Yu L, Wang Z, Yu W, Zhao C, Zhong S, Cui J, Shao K, Na H (2009) Polym Compos 30:948
27. Asif A, Lakshmana Rao V, Saseendran V, Ninan KN (2009) Polym Eng Sci 49:756
28. Zunjarrao SC, Sriraman R, Singh RP (2006) J Mater Sci 41:2219. doi:10.1007/s10853-006-7179-2
29. Bhattacharya M, Bhowmick AK (2010) J Mater Sci 45:6126. doi:10.1007/s10853-010-4699-6
30. Gilman JW, Jackson CL, Morgan AB, Harris R Jr (2000) Chem Mater 12:1866
31. Giannelis EP, Krisnamoorti RK, Manias E (1999) Adv Polym Sci 138:107
32. Alexandre M, Dubois P (2000) Mater Sci Eng Rep 28:1
33. Hu Y, Wang S, Ling Z, Zhuang Y, Chen Z, Fan W (2003) Macromol Mater Eng 288:272
34. Zanetti M, Camino G, Canavese D, Morgan AB, Lamelas FG, Wilkie CA (2002) Chem Mater 14:189
35. Seo KS, Kim DS (2006) Eng 46:1318
36. Brown J, Rhoney I, Pethrick RA (2004) Polym Int 53:2130

37. Zulfiqar S, Ahmad Z, Ilyas Sarwar M (2008) Polym Adv Technol 19:1720
38. Si M, Zaitsev V, Goldman M, Frenkel A, Peiffer DG, Weil E, Sokolov JC, Rafailovich MH (2007) Polym Degrad Stab 92:86
39. Zhu SW, Shi WF (2003) Polym Degrad Stab 80:217
40. Liu YL (2002) J Polym Sci A 40:359
41. Ravikrishnan A, Sudhakara P, Kannan P (2010) J Mater Sci 45:435. doi:10.1007/s10853-005-6930-4
42. Van Krevelen DW (1990) Properties of polymers. Elsevier, New York
43. Kornmann K, Lindberg H, Berglund LA (2001) Polymer 42:1303
44. Hedrick JL, Jurek MJ, Yilgor I, McGrath JE (1985) Polym Prepr 26:293